

bond angle to 113° or more. Second, the energy needed to distort the bond angle increases rather slowly and reaches values that compete with the steric hindrance only beyond 120°. Checking the energy barrier between the two minima at low bond angle, we found it to decrease from 13 to 7, 2.7 and 0.7 kJ/mol when going from  $\beta = 109.5^\circ$  to 110, 111, and 112°, respectively. A further feature of the calculation with different bond angles was to show that relaxing the restraining of  $G = -\bar{G}$  and  $T = 180^\circ$  does not lead to lower energy conformations at bond angles above 114° ( $\beta = 109.5^\circ$ ,  $\Delta E = 7$  kJ/mol;  $\beta = 110^\circ$ ,  $\Delta E = 2.5$  kJ/mol;  $\beta = 111^\circ$ ,  $\Delta E = 2.0$  kJ/mol;  $\beta = 112^\circ$ ,  $\Delta E = 1.8$  kJ/mol;  $\beta = 113^\circ$ ,  $\Delta E = 0.8$  kJ/mol;  $\beta = 114^\circ$ ,  $\Delta E = 0.3$  kJ/mol). As one would expect from these numbers, the minima above 112° for the bond angle  $\beta$  are rather shallow and rotation from  $\phi = 40^\circ$  to  $80^\circ$  shows a potential energy variation of less than 1 kJ/mol. Without intermolecular constraints by the crystal, the chain may thus assume practically any bond angle  $\beta$  between 112 and 118° and any torsional angle  $\phi$  between 40 and 80°. Table II shows that all of these conformations can also satisfy the repeat-length constraint (in any given pairs).

### Discussion

These conformation calculations indicate that poly(vinylidene fluoride) should have, at least at high temperatures, increased mobility, i.e., represent perhaps a condic crystal. Indeed, initial heat capacity analyses of crystalline poly(vinylidene fluoride)<sup>11</sup> seem to indicate an elevated heat capacity between the glass transition and the melting temperature when compared to the purely vibrational heat capacity of the solid.<sup>4</sup> There is, however, no indication of a first-order transition, as was observed for the polyethylene and poly(tetrafluoroethylene) crystal to condic crystal change or was reported for a Curie transition.<sup>3</sup>

Other experimental evidence that may be linked to conformational changes are a dielectric relaxation ( $\alpha_c$ ) above about 325 K, suggested to be due to TGT $\bar{G}$   $\rightarrow$  GT $\bar{G}$ T changes.<sup>12</sup> This would give rise to a change in the up and down orientation (inclination) of the -F bonds along the chain, as was observed by X-ray diffraction.<sup>13</sup>

At temperatures above 440 K, changes in the c projection of the chain were attributed to TGT $\bar{G}$   $\rightarrow$  GT $\bar{G}$ T conformational mobility.<sup>13,14</sup> At present, the question of the driving force of these conformational changes is not clear. It seems that intermolecular packing improvement through removal of domain boundaries may prevent reversal of once-induced changes.

At the addition to thermal motion of the electrical field needed for poling, the transformation TGT $\bar{G}$   $\rightarrow$  T $\bar{G}$ TG was proposed<sup>15</sup> as a conformation change, irreversible without the presence of a field. Partial loss of polarity is, however, observed before fusion,<sup>16</sup> so that conformational changes of the earlier described types may also contribute to the poling and reach their Curie temperature range before melting.

Finally, a rather large variability of X-ray structure data with sample<sup>3,17</sup> may point to easy changes in conformation with changes in intermolecular forces, the latter being induced by changes in the concentration of head-to-head sequences.

### Summary

Molecular mechanics calculations for isolated poly(vinylidene fluoride) molecules indicate a broad potential energy minimum permitting -C- bond angles between 112 and 118° and rotation angles between 40 and 80°. In the crystal, intermolecular packing considerations must limit the large-scale motion between the given limits. The un-

freezing to a conformationally disordered crystal (condic crystal) seems to occur in stages and be driven by intermolecular packing improvements or electric field induced poling strains. Full mobility as needed at the Curie temperature seems to be possible only above the melting temperature.

**Acknowledgment.** This work was supported by a grant from the National Science Foundation, Grant No. DMR 8317097.

**Registry No.** Poly(vinylidene fluoride), 24937-79-9.

### References and Notes

- (1) Wunderlich, B.; Grebowicz, J. *Adv. Polym. Sci.* **1984**, *60/61*, 1.
- (2) Kawai, H. *Jpn. J. Appl. Phys.* **1969**, *8*, 975.
- (3) Lovinger, A. J. *Polymer* **1983**, *24*, 1225, 1233. Furukawa, T.; Davis, G. T.; Broadhurst, M. G. *J. Appl. Phys.* **1984**, *56*, 2412. Green, J. S.; Rabe, J. P.; Rabolt, J. F. *Macromolecules*, submitted.
- (4) Loufakis, K.; Wunderlich, B. *Polymer* **1985**, *26*, 1875.
- (5) Miller, K. J.; Broadzinsky, R.; Hall, S. *Biopolymers* **1980**, *19*, 2091.
- (6) Hasegawa, R.; Takahashi, Y.; Chatani, Y.; Tadokoro, H. *Polym. J. (Tokyo)* **1972**, *3*, 591.
- (7) Farmer, B. L.; Hopfinger, A. J.; Lando, J. B. *J. Appl. Phys.* **1972**, *43*, 4293.
- (8) Bachmann, M. A.; Lando, J. B. *Macromolecules* **1981**, *14*, 40. Takahashi, Y.; Matsubara, Y.; Tadokoro, H. *Macromolecules* **1983**, *16*, 1588.
- (9) Westheimer, H. In "Steric Effects in Organic Chemistry"; Newman, M. S., Ed.; Wiley: New York, 1956; Chapter 12.
- (10) Tripathy, S. K.; Potenzzone, R., Jr.; Hopfinger, A. J.; Banik, N. C.; Taylor, P. L. *Macromolecules* **1979**, *12*, 656.
- (11) Loufakis, K.; Wunderlich, B. to be published.
- (12) Miyamoto, Y.; Miyaji, H.; Asai, K. *J. Polym. Sci., Polym. Phys. Ed.* **1980**, *18*, 597.
- (13) Takahashi, Y.; Miyaji, K. *Macromolecules* **1983**, *16*, 1789. Takahashi, Y.; Tadokoro, H. *Ferroelectrics* **1984**, *57*, 187. Takahashi, Y.; Tadokoro, H. *Macromolecules* **1983**, *16*, 1880.
- (14) Takahashi, Y. *Polym. J. (Tokyo)* **1983**, *15*, 733.
- (15) Lovinger, A. *Macromolecules* **1981**, *14*, 227.
- (16) Davis, G. T.; McKinney, J. E.; Broadhurst, J. E.; Roth, S. C. *J. Appl. Phys.* **1978**, *49*, 4998. Servet, B.; Rault, J. *J. Phys. (Les Ulis, Fr.)* **1979**, *40*, 1145.
- (17) Takahashi, Y.; Matsubara, Y.; Tadokoro, H. *Macromolecules* **1983**, *16*, 1588.
- (18) Miller, K. J.; Savchik, J. *J. Am. Chem. Soc.* **1979**, *101*, 7206.

### Small-Angle X-ray Investigation of Morphological Order in the System Isotactic Polystyrene-Poly(2,6-dimethylphenylene oxide)

W. WENIG,<sup>†</sup> W. J. MACKNIGHT, and F. E. KARASZ\*

*Polymer Science and Engineering Department, University of Massachusetts, Amherst, Massachusetts 01003. Received October 4, 1985*

Blends of isotactic polystyrene and poly(2,6-dimethylphenylene oxide) (PPO) can be crystallized by thermal treatment for PPO contents lower than 40%. The samples reveal crystallinities which vary from below 20% to just over 30%.<sup>1,2</sup>

Wide-angle X-ray diffraction results show curves typical for partially crystallized isotactic polystyrene, which suggests that the blends consist of a homogeneous amorphous phase and a discrete crystalline phase. It is concluded from the appearance of a long period in the small-angle X-ray scattering (SAXS) curves of the blends that the crystals are arranged in a partially ordered manner. In an earlier

<sup>†</sup>Laboratorium für Angewandte Physik, Universität Duisburg, 4100 Duisburg, West Germany.

paper<sup>2</sup> we showed that the SAXS curves of these blends can be calculated theoretically by use of Hosemann's model of the linear paracrystal.<sup>3-5</sup> This model proves to be a good approximation for systems with high correlation numbers ( $N \geq 10$ ); however, for low correlation, as in the present iPS/PPO blends ( $N \approx 2$ ), it may lead to false results. As was recently shown, the amorphous density as well as the mean sample density plays an important role.<sup>6</sup>

In this paper we present theoretical calculations using a model which recognizes the density contrast<sup>6</sup> and compare the calculated morphological parameters to those that had been derived from Hosemann's black-white model.

## Results

We first present results needed<sup>6</sup> for this analysis. Let  $\rho_c$  be the electron density of the crystals,  $\rho_a$  the electron density of the amorphous layers, and  $\rho_u$  the mean sample density. The intensity as a function of  $s$  ( $s = (2 \sin \theta)/\lambda$ ) is then given by

$$I(s) = \frac{1}{2\pi^2 s^2} \operatorname{Re} \left\{ \Delta\rho_i^2 \left[ N \frac{(1-f_x)(1-f_y)}{1-f_z} + f_y \frac{(1-f_x)^2}{(1-f_z)^2} (1-f_z N) \right] + \Delta\rho_u^2 (1-f_z^N) - \Delta\rho_i \Delta\rho_u \frac{1-f_x}{1-f_z} (1-f_z^N) \right\} \quad (1)$$

where  $\Delta\rho_i = \rho_c - \rho_a$ ,  $\Delta\rho_u = \rho_u - \rho_a$ , and  $f_x$  and  $f_y$  are the normalized thickness-distribution functions of the crystals and the amorphous layers:

$$f_x = \int_0^\infty H(x) e^{-2\pi i s x} dx$$

with a corresponding term for  $f_y$ , and

$$f_z = f_x f_y$$

Hosemann's "black-white" model results<sup>6</sup> from (1) by using the approximation

$$\Delta\rho_i = 1; \quad \Delta\rho_u = 0 \quad (\rho_c = 1, \rho_a = \rho_u = 0)$$

$$I(s) = \frac{1}{2\pi^2 s^2} \operatorname{Re} \left\{ N \frac{(1-f_x)(1-f_y)}{1-f_z} + f_y \frac{(1-f_x)^2}{(1-f_z)^2} (1-f_z^N) \right\} \quad (2)$$

Gaussian distribution functions had been used for both the lamellar and interlamellar thickness distributions. Mean sample densities of the partially crystallized and the amorphous samples have been measured by the density gradient method.

In Figure 1 the experimental SAXS curves for the blends of denoted composition are displayed together with various theoretical curves: the curves calculated by eq 1 and 2, respectively, and a curve calculated from eq 1 taking the best fit parameters obtained by using eq 2. A comparison of this curve with those calculated to give the best agreement with the experimental curves should provide an estimate of the validity of the "black-white" approximation. As Figure 1 shows, the black-white model is reasonably satisfactory for pure iPS but becomes more incorrect as the PPO content increases. Concurrently the correlation parameter (see below, Figure 4) decreases. This is in good agreement with earlier findings which state that the black-white model becomes increasingly invalid when the correlation of crystal lamellae decreases.

The crystal thicknesses (Figure 2), as well as the interlamellar distances (Figure 3), calculated from eq 1, appear lower than those calculated with eq 2. It has been questioned whether these small differences of the calculated values can be determined significantly. However, the

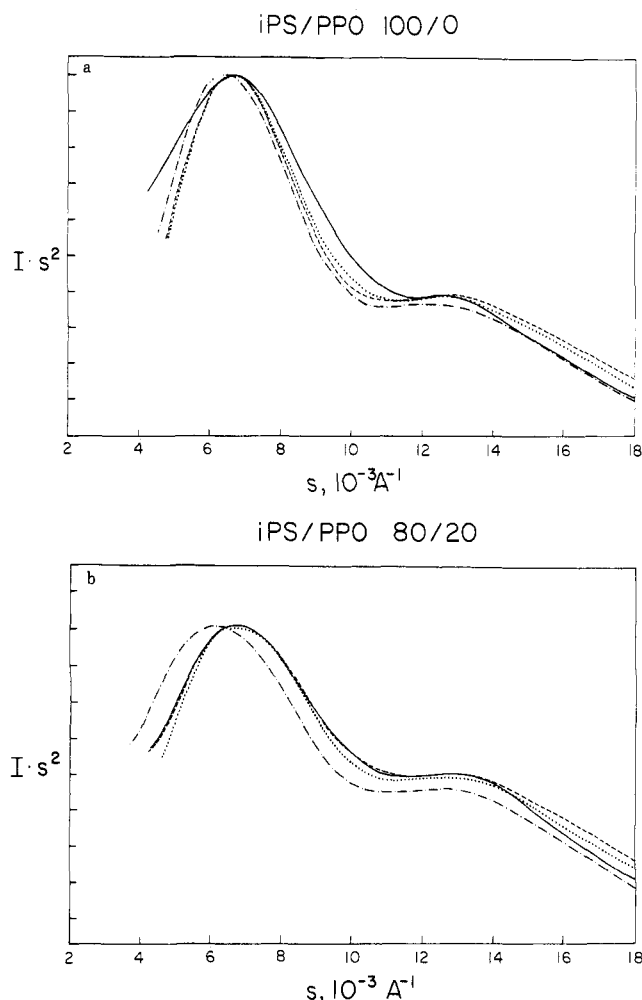


**Figure 1.** Small-angle X-ray scattering curves (Lorentz corrected) of pure iPS and a representative blend with composition as shown: (—) experimental curve; (---) best fit of the calculated curve using Hosemann's model; (···) best fit using the improved model; (-·-) curve calculated by use of the density model using the best fit parameters obtained with the Hosemann model. The mismatch of this curve shows the deviation between the two models.

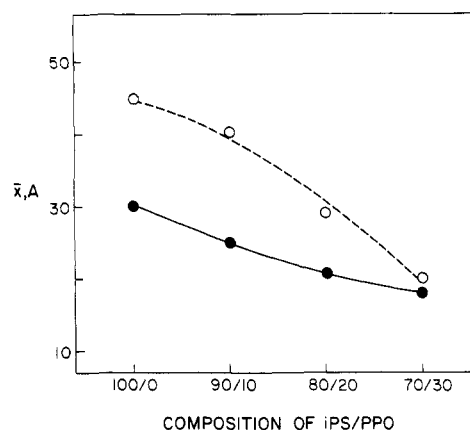


**Figure 2.** Mean thickness of crystal lamellae,  $\bar{x}$ . The solid curve is calculated from the improved model, the broken curve from Hosemann's model.

decrease of the values of the crystal thickness in the pure iPS amounts to 40%, which is a considerable difference. Furthermore, it has to be considered that the scattering curve is most sensitive to variations for  $N$  values between 1 and 2, because the scattering curve then changes from a gas scattering curve (diffuse scattering) to one which is produced by interparticle interference. As for low corre-

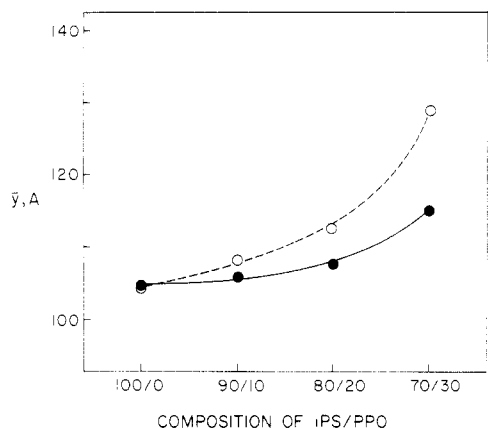


**Figure 3.** Mean thickness of the amorphous layers,  $\bar{y}$ . The solid curve is calculated from the improved model, the broken curve from Hosemann's model.

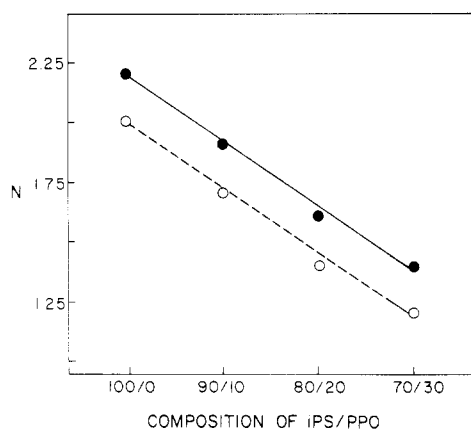


**Figure 4.** Average number of crystals in a stack calculated for both models (solid curve, improved model; broken curve, Hosemann's model).

lation of the crystals, clusters of crystal lamellae as well as crystals with no correlated neighbors will occur in the sample.

For crystallinities below 50% the shape of the scattering curve is determined primarily by the fluctuation of the interlamellar distance distribution function. To what extent lamellar twisting or similar dislocations of the supermolecular lattice leads to erroneous determinations of structure parameters cannot be concluded from these experiments alone. Evaluations of crystal size parameters from wide-angle X-ray scattering curves<sup>1</sup> yield values of the lamellar thicknesses of the same order of magnitude as the present results, and since there is no reason to assume the two models deal differently with the problem, we feel justified in discussing the parameters obtained at least qualitatively. Lamellar twisting, however, would primarily affect the correlation parameter  $N$ . Electron micrographs of iPS/PPO blends, obtained by the defocusing method,<sup>7</sup> show bundles of 3-4 lamellae per cluster. It is difficult to compare morphological parameters derived from electron micrographs to those calculated with a one-dimensional model; it seems, however, that the statistical parameter  $N$  does not exactly define the number of the lamellae stacked in a cluster. However, the results do indicate that in this system of imperfectly formed crystalline aggregates both models show, albeit somewhat qualitatively, that blending further lowers the apparent lamellar correlation.

The calculations show that for both models the correlation decreases with increasing PPO content (Figure 4). This is confirmed by electron microscopy, which seems to

show an even steeper decrease of this parameter.<sup>7</sup> The results show that the lamellar cluster model has to be used carefully when systems with a very low orientation correlation of the lamellae are investigated. Although the order of magnitude of the correlation parameters and their variation with sample composition can be obtained with some accuracy, no absolute values can be given.

**Acknowledgment.** F.E.K. thanks AFOSR for support through AFOSR Grant 84-0033.

**Registry No.** Isotactic polystyrene, 25086-18-4; PPO, 24938-67-8.

## References and Notes

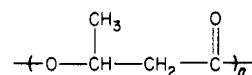
- (1) Hammel, R.; MacKnight, W. J.; Karasz, F. E. *J. Appl. Phys.* **1975**, *46*, 4199.
- (2) Wenig, W.; Karasz, F. E.; MacKnight, W. J. *J. Appl. Phys.* **1975**, *46*, 4194.
- (3) Hosemann, R. *Z. Phys.* **1939**, *114*, 10.
- (4) Hosemann, R.; Baghi, S. N. "Direct Analysis of Diffraction by Matter"; North-Holland Publishing Co.: Amsterdam, 1965.
- (5) Laue, M. V. "Röntgenstrahlinterferenzen"; Akad. Verlagsgesellschaft: Frankfurt/Main, 1960; Chapter 2.
- (6) Wenig, W.; Bramer, R. *Colloid Polym. Sci.* **1978**, *256*, 125.
- (7) Petermann, J., unpublished results.

## <sup>1</sup>H and <sup>13</sup>C NMR Analysis of Poly( $\beta$ -hydroxybutyrate) Isolated from *Bacillus megaterium*

YOSHIHARU DOI,\* MASAO KUNIOKA, YOSHIYUKI NAKAMURA, and KAZUO SOGA

Research Laboratory of Resources Utilization, Tokyo Institute of Technology, Nagatsuta, Midori-ku, Yokohama 227, Japan. Received October 25, 1985

Poly( $\beta$ -hydroxybutyrate) (PHB) is a naturally occurring polyester that is synthesized by the condensation of D-(-)- $\beta$ -hydroxybutyryl coenzyme A in a wide variety of bacteria.<sup>1-3</sup> The polymer is highly crystalline and optically active<sup>4</sup> and functions as both a source of energy and carbon supply for the bacteria.<sup>5</sup> Recently, PHB has attracted industrial attention as a possible candidate of the large-scale biotechnological products.<sup>6</sup> Infrared analysis, elemental analysis, and hydrolysis of the polymer have supported a linear head-to-tail polyester with the following formula:<sup>7-9</sup>



An X-ray fiber diagram of optically active PHB in the solid state showed a fiber repeat of 5.96 Å, corresponding to the length of two monomeric units ( $2_1$  helix).<sup>9,10</sup> The solution properties of PHB in several solvents have been studied by means of intrinsic viscosity, optical rotatory dispersion, and light scattering,<sup>11,12</sup> which indicate retention of the helical conformation in chloroform.

In this paper, we report <sup>1</sup>H and <sup>13</sup>C NMR spectra of PHB isolated from *Bacillus megaterium* and analyze the possible conformation of PHB in chloroform.

Figure 1 shows a proton-noise-decoupled <sup>13</sup>C NMR spectrum at 125 MHz of PHB in chloroform at 27 °C. Every peak of PHB is very sharp and only four lines remain. This result is consistent with that for a PHB containing regular head-to-tail sequences where all methyl, methylene, methine, and carbonyl carbons occupy struc-